

Phenotyping transgenic embryonic murine hearts using optical coherence tomography

Michael W. Jenkins, Pankti Patel, Huayun Deng, Monica M. Montano, Michiko Watanabe, and Andrew M. Rollins

We used optical coherence tomography (OCT) to characterize the morphological phenotype of embryonic murine hearts discerning hexamethylene-bis-acetamide-inducible protein 1 (HEXIM1) mutants from their wild-type littermates. At E12.5 and E13.5 murine embryos were excised from the mother, the hearts were removed, and 3D OCT data sets were obtained from each heart in the litter. Next, we segmented the morphological borders to obtain cavity volumes and wall thicknesses. The mutant hearts exhibited increased ventricular chamber volume and decreased compact myocardium wall thickness when compared with their wild-type littermates. Also, the E13.5 HEXIM1 $-/-$ embryo was distinguished by morphological asymmetry (underdeveloped left side). © 2007 Optical Society of America

OCIS codes: 170.4500, 170.3880, 100.68900, 110.4500.

1. Introduction

Manipulation of the genome has allowed researchers to identify mechanisms of disease and development. The mouse is currently a widely used animal model for genetic manipulations, because it is a mammal with a four-chambered heart, a short gestation period (20–21 days), and a completely mapped genome.¹ The transcription factor hexamethylene-*bis*-acetamide-inducible protein 1 (HEXIM1) is a tumor suppressor and a cyclin-dependent kinase inhibitor. Overexpression of HEXIM1 protein in breast cells results in decreased cell proliferation.^{2,3} HEXIM1 is expressed in murine heart tissues from embryonic day 10.5 and deletion of the C-terminal region of the HEXIM1 gene leads to perinatal death, growth retardation, abnormal coronary patterning, thin ventricular walls, and increased size of the ventricular cavities.^{4,5} These findings suggest HEXIM1 signaling regulates critical

pathways in coronary vessel patterning, myocardial vascularization, and ventricular compaction in the developing heart. To fully characterize the genesis of the defects in the HEXIM1 mutant mice, a tool capable of assessing structure and function simultaneously at early stages of development is needed. Pinpointing the time when the defect can be first detected is crucial to understanding the etiology of heart defects.

Optical coherence tomography (OCT)^{6,7} measures coherently gated backreflected light to image with resolutions of 2–15 μm to a depth of 1–2 mm in cardiac tissue. The high resolution and appropriate field of view have made OCT a worthy resource for the study of cardiac development. Boppart *et al.*⁸ imaged *Xenopus-laevis* hearts and were able to estimate ejection fraction by extrapolating the *M*-scan image data to a volume (assuming an ellipsoid-shaped ventricle). Yelbuz *et al.*⁹ imaged embryonic chick hearts in 2D (*in vivo*) and 3D (fixed). We obtained 4D images of embryonic chick hearts by pacing excised hearts and gating the image acquisition to the cardiac cycle.¹⁰ Recently, groups have imaged fixed embryonic murine hearts¹¹ and imaged paced excised embryonic murine hearts using gated OCT,¹⁰ but studies demonstrating the use of OCT imaging to compare genetically altered hearts to wild-type hearts is still lacking. Recently, genetically altered adult murine skeletal muscle was imaged with OCT.¹²

We demonstrate the first phenotyping of embryonic murine hearts using OCT. OCT was used to discern and quantify morphological differences be-

M. W. Jenkins (mwj5@case.edu), P. Patel, and A. M. Rollins are with the Department of Biomedical Engineering, Case Western Reserve University, 11100 Euclid Avenue, Cleveland, Ohio 44106. H. Deng and M. M. Montano are with the Department of Pharmacology, Case Western Reserve University School of Medicine, 2109 Adelbert Road, Cleveland, Ohio 44106. M. Watanabe is with the Department of Pediatrics, Case Western Reserve University School of Medicine, 11100 Euclid Avenue, Cleveland, Ohio 44106.

Received 30 June 2006; revised 26 October 2006; accepted 17 November 2006; posted 22 November 2006 (Doc. ID 72562); published 13 March 2007.

0003-6935/07/101776-06\$15.00/0

© 2007 Optical Society of America

tween embryonic murine hearts from HEXIM1 mutant mice and their wild-type littermates at E12.5 and E13.5 (12.5 and 13.5 days after fertilization). Compared to the wild types, the HEXIM1 mutant hearts showed increased ventricular chamber volumes and thinned compact myocardium. The E13.5 mutant displayed an asymmetrical morphology as the left ventricle and atrium both presented growth retardation. OCT offers a noninvasive solution to phenotyping and has the possibility of greater accuracy, when compared to histological techniques, by eliminating fixation artifacts. In the future OCT will have the extra benefit of making morphological and functional measurements simultaneously. Also, OCT has the potential to be a high-throughput screening tool for the determination of appropriate assays for further analysis.

2. Experimental Methods

A. Model Preparation and Imaging Protocol

HEXIM1 $-/-$ mice were created with an insertional mutation in the HEXIM1 gene that disrupts the C-terminal region. A mouse embryonic stem cell line XB322, which contained an insertional mutation in HEXIM1, was injected into C57BL/6 blastocysts. The blastocysts resulted in two chimeric male mice that were bred with C57BL/6 female mice (achieving germline transmission of the mutant allele).⁴ Mice are checked every morning for a vaginal plug, which indicates mating has occurred. The mouse embryo is considered to be E0.5 (0.5 days after fertilization) upon detection of the plug. Further refinement in staging is accomplished by examining the morphological features of the embryo and comparing them with the features at known stages.¹³

Between days 12 and 14 of development, the mother was euthanized, and the embryos were surgically removed from the uterus. The mother and embryos were warmed with a heating pad until just prior to imaging. The first embryo was removed from the umbilical cord, and the heart was dissected from the body. The excised heart was pinned to silicone between two platinum plates in a pacing chamber filled with oxygenated saline solution. The heart was pinned with the ventral surface facing up, which allowed for four-chambered *en face* OCT images. The hearts were paced at 1 Hz and imaged with a gated-OCT system developed in our laboratory.¹⁰ By using the gated-OCT system, we were able to capture a 3D data set of the heart in end relaxation. All subsequent measurements were made on the 3D data sets from the end-relaxation phase in the cardiac cycle. The process was repeated until all the littermates were imaged. The dissected hearts and body were placed in 10% formalin after imaging. The genotype was confirmed with a three-primer polymerase chain reaction from DNA taken from the tail of each embryo. All the littermates were imaged a second time after fixation. The results include data collected from two litters of mice at two stages of development (E12.5 and E13.5). The E12.5 litter contained one mutant,

one wild type, and four heterozygotes, while the E13.5 litter contained one mutant, one wild type, and two heterozygotes.

Our gated-OCT system consists of a time-domain OCT system capable of capturing 4000 A scans per second,¹⁴ a field-programmable gate array to gate image acquisition and a microscope-integrated OCT scanner allowing visual verification of the imaging location.¹⁵ The coherence function of our light source (which determines the axial resolution) was 14 μm FWHM in air, while the intensity profile of the incident beam (which determines the transverse resolution) was measured as 10 μm FWHM. Imaging time varied between 5 and 10 min depending on the specimen.

With these specifications, we are able to generate 4D images from 16 phases of the cardiac cycle, thereby providing the potential of collecting functional data (e.g., ejection fraction) during contraction and relaxation. Parameters that have significant influences on cardiac contraction were not controlled in these experiments (oxygen levels, preload and afterload conditions). For this reason, we focused on morphological measurements on 3D images at end relaxation.

B. Image Analysis

All 3D image sets were visualized and evaluated using ANALYZE 6.0 (Mayo Clinic) and MATLAB 7.0 (Mathworks, Inc.). To prepare the images for segmentation and quantitative analysis, we averaged five images at each position, applied a median filter, and corrected the aspect ratio. Two-dimensional OCT images were viewed in the *en face* orientation to allow all four chambers to be visible simultaneously. Three-dimensional OCT images were assembled using surface rendering or volume compositing. Figure 1 shows a typical presentation of an E13.5 wild-type murine heart, including a 3D surface rendering, a microscope image and an *en face* 2D OCT image. The accurate morphological representation and exquisite detail provided by OCT imaging is readily observed.

Of the six embryonic hearts from the E12.5 litter and the four from the E13.5 litter, only one mutant and one wild type from each litter were present. Because of the various permutations of the heterozygous hearts, we focused on analyzing the one mutant and one wild-type heart at each stage to assess the effect of the HEXIM1 gene on heart development. To characterize the HEXIM1 mutants from the wild types, we measured the volumes and wall thicknesses of the atria and ventricles. The left and right atrial cavities and outer walls were segmented manually. The inner volumes of the atria were calculated by summing the number of voxels in each 2D slice. To make wall measurements of the E13.5 atria, radial lines were drawn out from the center of the cavity, and the distance that each line intersected with the wall was measured as shown in Fig. 2(a). The radial line approximation is valid for circular and ellipsoid-shaped cavities as was the case for the E13.5 mice. Each radial line was inspected and included only if it adequately approximated the wall thickness (e.g.,

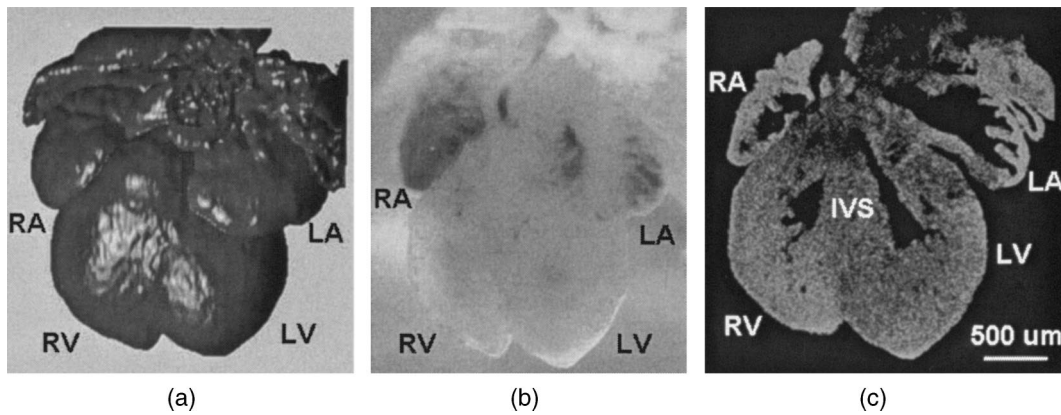


Fig. 1. E13.5 wild-type embryonic murine heart: 3D surface rendering reconstructed from (a) OCT data, (b) video microscope image, and (c) 2D *en face* OCT image. RA, right atrium; RV, right ventricle; LA, left atrium; LV, left ventricle; and IVS, interventricular septum.

excluded any folded regions or segments that were not perpendicular with the inner and outer wall borders) and an average wall thickness (>40 measurements) was determined over multiple slices. For the E12.5 atria, the cavities included a myriad of folds, and we manually determined the intersection lines and averaged (>40 measurements) the length of mul-

iple intersection lines as in the E13.5 mice [shown in Fig. 2(b)].

Measurements on the ventricles were complicated by the fact that the ventricular cavities of the embryonic murine heart are largely filled with trabecular tissue. Since the left ventricle in the E13.5 mutant was underdeveloped and lacked a cavity, we com-

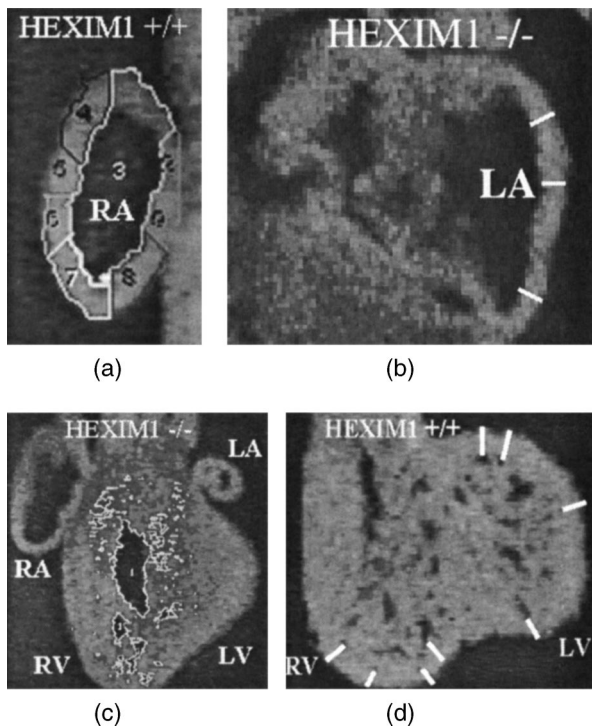


Fig. 2. Illustration of morphological measurement techniques. (a) Atrial wall thickness measurements were made using radial lines. Radial lines are drawn outward from a center point in the atrial cavity and the length of the intersection with the wall is computed. (b) For nonspherical or elliptical atria, wall thickness was measured manually. (c) Ventricular volumes were measured using thresholding and voxel counting. (d) Compact myocardial thickness was measured by manually determining the distance from outer trabecular spaces to the outer surface of the ventricles. RA, right atrium; RV, right ventricle; LA, left atrium; and LV, left ventricle.

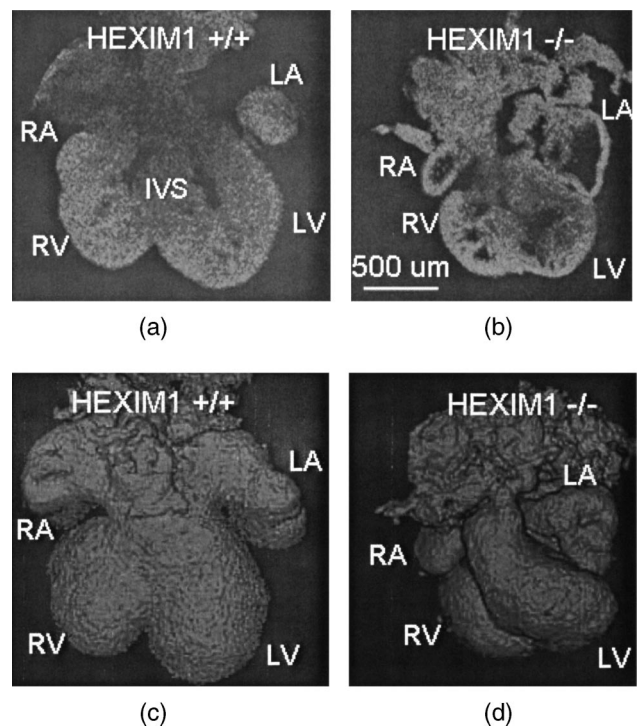


Fig. 3. E12.5 HEXIM1 mutant heart versus its wild-type littermate. (a) Two-dimensional *en face* OCT image of the HEXIM1 wild-type heart. (b) Two-dimensional *en face* OCT image of the HEXIM1 mutant murine heart. Enlarged ventricular cavities and thinned compact myocardium are evident in the 2D image. (c) Three-dimensional volume composite image reconstructed from OCT data of the wild-type heart. (d) Three-dimensional volume composite image reconstructed from OCT data of the mutant heart. Mutant heart appears to be smaller and younger developmentally. RA, right atrium; RV, right ventricle; LV, left ventricle; LA, left atrium; and IVS, interventricular septum.

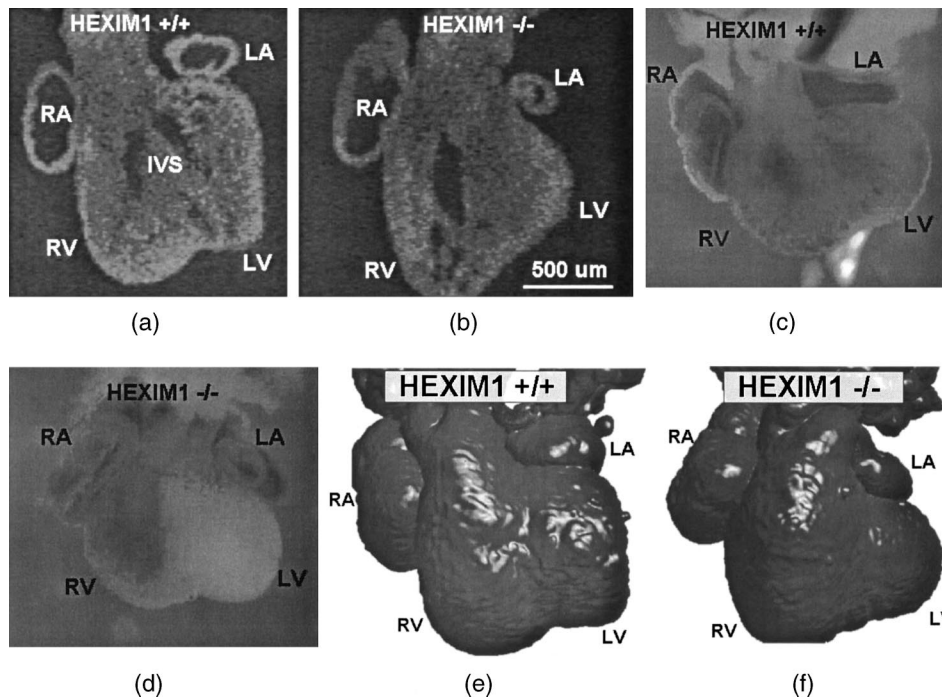


Fig. 4. E13.5 HEXIM1 mutant heart versus its wild-type littermate. (a) Two-dimensional *en face* OCT image of the HEXIM1 wild-type heart. One can clearly see the interventricular septum, which is absent in the transgenic heart. (b) Two-dimensional *en face* OCT image of the HEXIM1 mutant murine heart. Left atrium is much smaller than in the wild type and the left ventricle is not fully formed (no cavity), while the cavity in the right ventricle is enlarged. (c) Video microscope image of the wild-type heart prior to OCT imaging. (d) Video microscope image of the transgenic heart prior to OCT imaging. Note the absence of blood in the left ventricle (no cavity). (e) Three-dimensional surface rendering reconstructed from OCT data of the wild-type heart. (f) Three-dimensional surface rendering reconstructed from OCT data of the mutant heart. RA, right atrium; RV, right ventricle; LV, left ventricle; LA, left atrium; and IVS, interventricular septum.

pared the combined ventricular volumes (right and left). The cavity volume was determined by selecting the image region entirely containing the cavity and thresholding to segment the empty spaces between trabeculations. The threshold was manually adjusted as a function of signal strength. Exponentially corrected images, which adjusted for the attenuation of light, were used to help determine threshold levels. The white tracings in Fig. 2(c) demarcate the open space of the ventricular cavity. Volumes were determined by summing the number of voxels representing open space in each 2D slice. Finally, the thickness of the compact myocardium was assessed by computing the length of the shortest lines connecting the outermost visible cavity spaces between trabeculations to the surface of the heart, as in Fig. 2(d). The average compact myocardial thickness was evaluated by averaging the length of lines (>40) from several 2D slices.

3. Results

A. Imaging

Figure 3 presents 2D and 3D images of a mutant and wild-type embryonic murine heart at E12.5. From the 2D images the mutant heart appears to have larger ventricular cavities and a thinner compact myocardium. The mutant heart is smaller and seems to be less developed compared with the wild type. Figure 4

shows a 2D OCT image, photograph, and 3D surface rendering of the E13.5 mutant heart [(a), (c), and (e)] compared to the wild type [(b), (d), and (f)]. The mutant heart is very asymmetrical as the left ventricle and atrium are underdeveloped (no cavity in ventricle and both are much smaller). The interventricular septum can clearly be seen in the wild type, but is absent in the mutant. The left ventricular cavity of the mutant appears enlarged in comparison with the wild type.

B. Measurements

Ventricular and atrial cavity volumes, atrial wall thicknesses, and compact myocardium thicknesses were measured to distinguish HEXIM1 mutant hearts from wild-type littermate hearts at stages E12.5 and

Table 1. Physiological Parameters of the Atria^a

Stage of Development	Right Atrial Wall Thickness (%)	Left Atrial Wall Thickness (%)	Right Atrial Volume (%)	Left Atrial Volume (%)
E12.5	71	58	39	47
E13.5	150	132	84	30

^a[(HEXIM1 -/- measurements)/(HEXIM1 +/- measurements)] × 100.

Table 2. Physiological Parameters of the Ventricle^a

Stage of Development	Combined Ventricular Volume (%)	Compact Myocardium Thickness (%)
E12.5	240	50
E13.5	286	89

^a[(HEXIM1 -/- measurements)/(HEXIM1 +/- measurements)] × 100.

E13.5. Atrial volumes of the mutant hearts were on average half the size of their wild-type littermates. The E12.5 mutant heart had a thicker atrial wall thickness, whereas the E13.5 mutant had a thinner atrial wall thickness. These measurements on the atria are summarized in Table 1. The ventricular volumes of the mutant hearts were more than twice the size of those of the wild-type littermates. The compact myocardium of the mutant ventricles was thinner than that of the wild-type ventricles. Table 2 summarizes these measurements on the ventricles.

4. Discussion and Conclusions

Our ventricular measurements are consistent with other techniques used to study HEXIM1 mutant hearts [ultrasound biomicroscopy (UBM) and standard histology] and include thinning of the compact myocardium and increased ventricular chamber size.^{4,5} These previous studies were qualitative and lacked any conclusive observations on the atria. Tables 1 and 2 summarize the results that were confirmed with these techniques and prove OCT's ability to phenotype embryonic murine hearts. As opposed to UBM, OCT's resolution enables one to image younger embryos with greater detail, whereas ultrasound is likely more fitting for older embryos. OCT has a suitable field of view and resolution for imaging embryonic hearts E8–E14, the critical period when the heart transforms from a peristaltic tube to a four-chambered heart. Also, this technique is nondestructive, potentially permitting longitudinal investigations, and free from artifacts of fixation. OCT can function as a high-throughput screening tool in order to determine the appropriate assays for further analysis.

A thin compact myocardium and enlarged ventricular chambers is consistent with dilated cardiomyopathy (DCM). Etiologies leading to DCM are varied, but studies have shown decreased vascular endothelial growth factor (VEGF) levels are linked to DCM.^{16,17} Decreased VEGF levels were found in HEXIM1 mutant embryonic mice.⁵

Our results demonstrate the viability of OCT for phenotyping embryonic murine hearts. Future plans include developing improved algorithms for automatically determining volumes and wall thicknesses, investigating a statistically relevant number of HEXIM1 and other mutants at various stages of development, and maintaining the environment of the hearts to enable physiologically relevant functional measurements (e.g., ejection fraction) using gated OCT. Maintaining

a physiologically relevant environment includes controlling oxygen levels and maintaining a physiologic pacing rate, using point stimulation instead of field stimulation, and controlling the preload and afterload conditions. The ability of OCT to discern morphological differences between viable embryonic mutant and wild-type hearts nondestructively can be a valuable tool to investigate mechanisms causing cardiac malformations.

The authors acknowledge that the work was conducted in a facility constructed with support from the Research Facilities Improvement Program C06 RR1246-01 from the National Center for Research Resources, National Institutes of Health (NIH). Support for the work also came from NIH grant CA92440 and a Case Western Reserve University startup grant. The authors thank Debashish Roy for image processing advice and Yong Qui Doughman for help with dissection.

References and Notes

1. W. F. Dietrich, J. Miller, R. Steen, M. A. Merchant, D. Damron-Boles, Z. Husain, R. Dredge, M. J. Daly, K. A. Ingalls, and T. J. O'Connor, "A comprehensive genetic map of the mouse genome," *Nature* **380**, 149–152 (1996).
2. B. M. Wittmann, N. Wang, and M. M. Montano, "Identification of a novel inhibitor of breast cell growth that is down-regulated by estrogens and decreased in breast tumors," *Cancer Res.* **63**, 5151–5158 (2003).
3. B. M. Wittmann, K. Fujinaga, H. Deng, N. Ogba, and M. M. Montano, "The breast cell growth inhibitor, estrogen down regulated gene 1, modulates a novel functional interaction between estrogen receptor alpha and transcriptional elongation factor cyclin T1," *Oncogene* **24**, 5576–5588 (2005).
4. H. Deng, Y. Doughman, L. Chaplin, M. Watanabe, and M. M. Montano, "A critical role for HEXIM1 in heart development," *FASEB J.* **20**:A1304-a (2006).
5. H. Deng, Y. Doughman, L. Chaplin, C. Padro, A. Koch, N. Wang, N. Ward, M. Watanabe, and M. M. Montano are preparing a paper to be called "Disruption of HEXIM1 gene: effects on heart and vascular development."
6. D. Huang, E. A. Swanson, C. P. Lin, J. S. Schuman, W. G. Stinson, W. Chang, M. R. Hee, T. Flotte, K. Gregory, C. A. Puliafito, and J. G. Fujimoto, "Optical coherence tomography," *Science* **254**, 1178–1181 (1991).
7. A. F. Fercher, W. Drexler, C. K. Hitzenberger, and T. Lasser, "Optical coherence tomography—principles and applications," *Rep. Prog. Phys.* **66**, 1–239 (2003).
8. S. A. Boppart, G. J. Tearney, B. E. Bouma, J. F. Southern, M. E. Brezinski, and J. G. Fujimoto, "Noninvasive assessment of the developing *Xenopus* cardiovascular system using optical coherence tomography," *Proc. Natl. Acad. Sci. U.S.A.* **94**, 4256–4261 (1997).
9. T. M. Yelbuz, M. A. Choma, L. Thrane, M. L. Kirby, and J. A. Izatt, "Optical coherence tomography a new high-resolution imaging technology to study cardiac development in chick embryos," *Circulation* **106**, 2771–2774 (2002).
10. M. W. Jenkins, F. Rothenberg, D. Roy, Z. Hu, V. P. Nikolski, M. Watanabe, D. L. Wilson, I. R. Efimov, and A. M. Rollins, "4D embryonic cardiography using gated optical coherence tomography," *Opt. Express* **14**, 736–748 (2006).
11. W. Luo, D. L. Marks, T. S. Ralston, and S. A. Boppart, "Three-dimensional optical coherence tomography of the embryonic murine cardiovascular system," *J. Biomed. Opt.* **11**, 021014 (2006).

12. J. J. Pasquesi, S. C. Schlachter, M. D. Boppart, E. Chaney, S. J. Kaufman, and S. A. Boppart, "In vivo detection of exercise-induced ultrastructural changes in genetically-altered murine skeletal muscle using polarization-sensitive optical coherence tomography," *Opt. Express* **14**, 1547–1556 (2006).
13. M. H. Kaufman, *The Atlas of Mouse Development* (Academic, 1998).
14. A. M. Rollins, S. Yazdanfar, M. Kulkarni, R. Ung-Arunyawee, and J. Izatt, "In vivo video rate optical coherence tomography," *Opt. Express* **3**, 219–229 (1998).
15. Z. Hu and A. M. Rollins, "Quasi-telecentric optical design of a microscope-compatible OCT scanner," *Opt. Express* **13**, 6407–6415 (2005).
16. P. Carmeliet, Y. S. Ng, D. Nuyens, G. Theilmeier, K. Brusselmans, I. Cornelissen, E. Ehler, V. V. Kakkar, I. Stalmans, V. Mattot, J. C. Perriard, M. Dewerchin, W. Flameng, A. Nagy, E. Lupu, L. Moons, D. Collen, P. A. D'Amore, and D. T. Shima, "Impaired myocardial angiogenesis and ischemic cardiomyopathy in mice lacking the vascular endothelial growth factor isoforms VEGF164 and VEGF188," *Nat. Med.* **5**, 495–502 (1999).
17. D. Abraham, R. Hofbauer, R. Schafer, R. Blumer, P. Paulus, A. Miksovsky, H. Traxler, A. Kocher, and S. Aharinejad, "Selective downregulation of VEGF-A(165), VEGF-R(1), and decreased capillary density in patients with dilative but not ischemic cardiomyopathy," *Circ. Res.* **87**, 644–647 (2000).